EUROPEAN ORGANIZATION FOR NUCLEAR RESEARCH

CERN–EP-2000-030

16 February 2000

# Determination of $|V_{ub}|/|V_{cb}|$ with DELPHI at LEP

DELPHI Collaboration

**Abstract**

The ratio of the CKM quark-mixing matrix elements $|V_{ub}|/|V_{cb}|$ has been measured using $B$ hadron semileptonic decays. The analysis uses the reconstructed mass $M_X$ of the secondary hadronic system produced in association with an identified lepton. Since $B \to X_u \ell \bar{\nu}$ transitions are characterised by hadronic masses below those of the $D$ mesons produced in $B \to X_c \ell \bar{\nu}$ transitions, events with a reconstructed value of $M_X$ significantly below the $D$ mass are selected. Further signal enrichments are obtained using the topology of reconstructed decays and hadron identification. A fit to the numbers of decays in the $b \to u$ enriched and depleted samples with $M_X$ above and below 1.6 GeV/$c^2$ and to the shapes of the lepton energy distribution in the $B$ rest frame gives $|V_{ub}|/|V_{cb}| = 0.103^{+0.011}_{-0.012}$ (stat.) $\pm$ 0.016 (syst.) $\pm$ 0.010 (model) and, correspondingly, a charmless semileptonic $B$ decay branching fraction of $\mathrm{BR}(B \to X_u \ell \bar{\nu}) = (1.57 \pm 0.35$ (stat.) $\pm 0.48$ (syst.) $\pm 0.27$ (model)$) \times 10^{-3}$.

(Accepted by Phys.Lett.B)

P.Abreu[22], W.Adam[52], T.Adye[38], P.Adzic[12], Z.Albrecht[18], T.Alderweireld[2], G.D.Alekseev[17], R.Alemany[51], T.Allmendinger[18], P.P.Allport[23], S.Almehed[25], U.Amaldi[9,29], N.Amapane[47], S.Amato[49], E.G.Anassontzis[3], P.Andersson[46], A.Andreazza[9], S.Andringa[22], P.Antilogus[26], W-D.Apel[18], Y.Arnoud[9], B.Åsman[46], J-E.Augustin[26], A.Augustinus[9], P.Baillon[9], P.Bambade[20], F.Barao[22], G.Barbiellini[48], R.Barbier[26], D.Y.Bardin[17], G.Barker[18], A.Baroncelli[40], M.Battaglia[16], M.Baubillier[24], K-H.Becks[54], M.Begalli[6], A.Behrmann[54], P.Beilliere[8], Yu.Belokopytov[9], K.Belous[44], N.C.Benekos[33], A.C.Benvenuti[5], C.Berat[15], M.Berggren[24], D.Bertrand[2], M.Besancon[41], M.Bigi[47], M.S.Bilenky[17], M-A.Bizouard[20], D.Bloch[10], H.M.Blom[32], M.Bonesini[29], M.Boonekamp[41], P.S.L.Booth[23], A.W.Borgland[4], G.Borisov[20], C.Bosio[43], O.Botner[50], E.Boudinov[32], B.Bouquet[20], C.Bourdarios[20], T.J.V.Bowcock[23], I.Boyko[17], I.Bozovic[12], M.Bozzo[14], M.Bracko[45], P.Branchini[40], R.A.Brenner[50], P.Bruckman[9], J-M.Brunet[8], L.Bugge[34], T.Buran[34], B.Buschbeck[52], P.Buschmann[54], S.Cabrera[51], M.Caccia[28], M.Calvi[29], T.Camporesi[9], V.Canale[39], F.Carena[9], L.Carroll[23], C.Caso[14], M.V.Castillo Gimenez[51], A.Cattai[9], F.R.Cavallo[5], V.Chabaud[9], M.Chapkin[44], Ph.Charpentier[9], P.Checchia[37], G.A.Chelkov[17], R.Chierici[47], P.Chliapnikov[9,44], P.Chochula[7], V.Chorowicz[26], J.Chudoba[31], K.Cieslik[19], P.Collins[9], R.Contri[14], E.Cortina[51], G.Cosme[20], F.Cossutti[9], H.B.Crawley[1], D.Crennell[38], S.Crepe[15], G.Crosetti[14], J.Cuevas Maestro[35], S.Czellar[16], M.Davenport[9], W.Da Silva[24], G.Della Ricca[48], P.Delpierre[27], N.Demaria[9], A.De Angelis[48], W.De Boer[18], C.De Clercq[2], B.De Lotto[48], A.De Min[37], L.De Paula[49], H.Dijkstra[9], L.Di Ciaccio[9,39], J.Dolbeau[8], K.Doroba[53], M.Dracos[10], J.Drees[54], M.Dris[33], A.Duperrin[26], J-D.Durand[9], G.Eigen[4], T.Ekelof[50], G.Ekspong[46], M.Ellert[50], M.Elsing[9], J-P.Engel[10], M.Espirito Santo[9], G.Fanourakis[12], D.Fassouliotis[12], J.Fayot[24], M.Feindt[18], A.Ferrer[51], E.Ferrer-Ribas[20], F.Ferro[14], S.Fichet[24], A.Firestone[1], U.Flagmeyer[54], H.Foeth[9], E.Fokitis[33], F.Fontanelli[14], B.Franek[38], A.G.Frodesen[4], R.Fruhwirth[52], F.Fulda-Quenzer[20], J.Fuster[51], A.Galloni[23], D.Gamba[47], S.Gamblin[20], M.Gandelman[49], C.Garcia[51], C.Gaspar[9], M.Gaspar[49], U.Gasparini[37], Ph.Gavillet[9], E.N.Gazis[33], D.Gele[10], N.Ghodbane[26], I.Gil[51], F.Glege[54], R.Gokieli[9,53], B.Golob[9,45], G.Gomez-Ceballos[42], P.Goncalves[22], I.Gonzalez Caballero[42], G.Gopal[38], L.Gorn[1], Yu.Gouz[44], V.Gracco[14], J.Grahl[1], E.Graziani[40], P.Gris[41], G.Grosdidier[20], K.Grzelak[53], J.Guy[38], C.Haag[18], F.Hahn[9], S.Hahn[54], S.Haider[9], A.Hallgren[50], K.Hamacher[54], J.Hansen[34], F.J.Harris[36], V.Hedberg[9,25], S.Heising[18], J.J.Hernandez[51], P.Herquet[2], H.Herr[9], T.L.Hessing[36], J.-M.Heuser[54], E.Higon[51], S-O.Holmgren[46], P.J.Holt[36], S.Hoorelbeke[2], M.Houlden[23], J.Hrubec[52], M.Huber[18], K.Huet[2], G.J.Hughes[23], K.Hultqvist[9,46], J.N.Jackson[23], R.Jacobsson[9], P.Jalocha[19], R.Janik[7], Ch.Jarlskog[25], G.Jarlskog[25], P.Jarry[41], B.Jean-Marie[20], D.Jeans[36], E.K.Johansson[46], P.Jonsson[26], C.Joram[9], P.Juillot[10], L.Jungermann[18], F.Kapusta[24], K.Karafasoulis[12], S.Katsanevas[26], E.C.Katsoufis[33], R.Keranen[18], G.Kernel[45], B.P.Kersevan[45], B.A.Khomenko[17], N.N.Khovanski[17], A.Kiiskinen[16], B.King[23], A.Kinvig[23], N.J.Kjaer[9], O.Klapp[54], H.Klein[9], P.Kluit[32], P.Kokkinias[12], V.Kostioukhine[44], C.Kourkoumelis[3], O.Kouznetsov[41], M.Krammer[52], E.Kriznic[45], Z.Krumstein[17], P.Kubinec[7], J.Kurowska[53], K.Kurvinen[16], J.W.Lamsa[1], D.W.Lane[1], V.Lapin[44], J-P.Laugier[41], R.Lauhakangas[16], G.Leder[52], F.Ledroit[15], V.Lefebure[2], L.Leinonen[46], A.Leisos[12], R.Leitner[31], G.Lenzen[54], V.Lepeltier[20], T.Lesiak[19], M.Lethuillier[41], J.Libby[36], W.Liebig[54], D.Liko[9], A.Lipniacka[9,46], I.Lippi[37], B.Loerstad[25], J.G.Loken[36], J.H.Lopes[49], J.M.Lopez[42], R.Lopez-Fernandez[15], D.Loukas[12], P.Lutz[41], L.Lyons[36], J.MacNaughton[52], J.R.Mahon[6], A.Maio[22], A.Malek[54], T.G.M.Malmgren[46], S.Maltezos[33], V.Malychev[17], F.Mandl[52], J.Marco[42], R.Marco[42], B.Marechal[49], M.Margoni[37], J-C.Marin[9], C.Mariotti[9], A.Markou[12], C.Martinez-Rivero[20], F.Martinez-Vidal[51], S.Marti i Garcia[9], J.Masik[13], N.Mastroyiannopoulos[12], F.Matorras[42], C.Matteuzzi[29], G.Matthiae[39], F.Mazzucato[37], M.Mazzucato[37], M.Mc Cubbin[23], R.Mc Kay[1], R.Mc Nulty[23], G.Mc Pherson[23], C.Meroni[28], W.T.Meyer[1], E.Migliore[9], L.Mirabito[26], W.A.Mitaroff[52], U.Mjoernmark[25], T.Moa[46], M.Moch[18], R.Moeller[30], K.Moenig[9,11], M.R.Monge[14], D.Moraes[49], X.Moreau[24], P.Morettini[14], G.Morton[36], U.Mueller[54], K.Muenich[54], M.Mulders[32], C.Mulet-Marquis[15], R.Muresan[25], W.J.Murray[38], B.Muryn[19], G.Myatt[36], T.Myklebust[34], F.Naraghi[15], M.Nassiakou[12], F.L.Navarria[5], S.Navas[51], K.Nawrocki[53], P.Negri[29], N.Neufeld[9], R.Nicolaidou[41], B.S.Nielsen[30], P.Niezurawski[53], M.Nikolenko[10,17], V.Nomokonov[16], A.Nygren[25], V.Obraztsov[44], A.G.Olshevski[17], A.Onofre[22], R.Orava[16], G.Orazi[10], K.Osterberg[16], A.Ouraou[41], M.Paganoni[29], S.Paiano[5], R.Pain[24], R.Paiva[22], J.Palacios[36], H.Palka[19], Th.D.Papadopoulou[9,33], K.Papageorgiou[12], L.Pape[9], C.Parkes[9], F.Parodi[14], U.Parzefall[23], A.Passeri[40], O.Passon[54], T.Pavel[25], M.Pegoraro[37], L.Peralta[22], M.Pernicka[52], A.Perrotta[5], C.Petridou[48], A.Petrolini[14], H.T.Phillips[38], F.Pierre[41], M.Pimenta[22], E.Piotto[28], T.Podobnik[45], M.E.Pol[6], G.Polok[19], P.Poropat[48], V.Pozdniakov[17], P.Privitera[39], N.Pukhaeva[17], A.Pullia[29], D.Radojicic[36], S.Ragazzi[29], H.Rahmani[33], J.Rames[13], P.N.Ratoff[21], A.L.Read[34], P.Rebecchi[9], N.G.Redaelli[29], M.Regler[52], J.Rehn[18], D.Reid[32], R.Reinhardt[54], P.B.Renton[36], L.K.Resvanis[3], F.Richard[20], J.Ridky[13], G.Rinaudo[47], I.Ripp-Baudot[10], O.Rohne[34], A.Romero[47], P.Ronchese[37], E.I.Rosenberg[1], P.Rosinsky[7], P.Roudeau[20], T.Rovelli[5], Ch.Royon[41], V.Ruhlmann-Kleider[41], A.Ruiz[42], H.Saarikko[16], Y.Sacquin[41], A.Sadovsky[17], G.Sajot[15], J.Salt[51], D.Sampsonidis[12], M.Sannino[14], Ph.Schwemling[24], B.Schwering[54], U.Schwickerath[18], F.Scuri[48], P.Seager[21], Y.Sedykh[17], A.M.Segar[36], N.Seibert[18], R.Sekulin[38], R.C.Shellard[6], M.Siebel[54], L.Simard[41], F.Simonetto[37], A.N.Sisakian[17], G.Smadja[26], O.Smirnova[25], G.R.Smith[38], A.Sokolov[44], O.Solovianov[44], A.Sopczak[18], R.Sosnowski[53], T.Spassov[22], E.Spiriti[40], S.Squarcia[14], C.Stanescu[40], S.Stanic[45], M.Stanitzki[18], K.Stevenson[36], A.Stocchi[20], J.Strauss[52], R.Strub[10], B.Stugu[4], M.Szczekowski[53], M.Szeptycka[53], T.Tabarelli[29], A.Taffard[23], F.Tegenfeldt[50], F.Terranova[29], J.Thomas[36], J.Timmermans[32], N.Tinti[5], L.G.Tkatchev[17], M.Tobin[23], S.Todorova[9], A.Tomaradze[2], B.Tome[22], A.Tonazzo[9], L.Tortora[40], P.Tortosa[51], G.Transtromer[25], D.Treille[9], G.Tristram[8], M.Trochimczuk[53], C.Troncon[28], M-L.Turluer[41], I.A.Tyapkin[17],

S.Tzamarias[12], O.Ullaland[9], V.Uvarov[44], G.Valenti[9,5], E.Vallazza[48], C.Vander Velde[2], P.Van Dam[32], W.Van den Boeck[2], W.K.Van Doninck[2], J.Van Eldik[9,32], A.Van Lysebetten[2], N.van Remortel[2], I.Van Vulpen[32], G.Vegni[28], L.Ventura[37], W.Venus[38,9], F.Verbeure[2], P.Verdier[26], M.Verlato[37], L.S.Vertogradov[17], V.Verzi[28], D.Vilanova[41], L.Vitale[48], E.Vlasov[44], A.S.Vodopyanov[17], G.Voulgaris[3], V.Vrba[13], H.Wahlen[54], C.Walck[46], A.J.Washbrook[23], C.Weiser[9], D.Wicke[54], J.H.Wickens[2], G.R.Wilkinson[36], M.Winter[10], M.Witek[19], G.Wolf[9], J.Yi[1], O.Yushchenko[44], A.Zaitsev[44], A.Zalewska[19], P.Zalewski[53], D.Zavrtanik[45], E.Zevgolatakos[12], N.I.Zimin[17,25], A.Zintchenko[17], Ph.Zoller[10], G.C.Zucchelli[46], G.Zumerle[37]

[1] Department of Physics and Astronomy, Iowa State University, Ames IA 50011-3160, USA
[2] Physics Department, Univ. Instelling Antwerpen, Universiteitsplein 1, B-2610 Antwerpen, Belgium
and IIHE, ULB-VUB, Pleinlaan 2, B-1050 Brussels, Belgium
and Faculté des Sciences, Univ. de l'Etat Mons, Av. Maistriau 19, B-7000 Mons, Belgium
[3] Physics Laboratory, University of Athens, Solonos Str. 104, GR-10680 Athens, Greece
[4] Department of Physics, University of Bergen, Allégaten 55, NO-5007 Bergen, Norway
[5] Dipartimento di Fisica, Università di Bologna and INFN, Via Irnerio 46, IT-40126 Bologna, Italy
[6] Centro Brasileiro de Pesquisas Físicas, rua Xavier Sigaud 150, BR-22290 Rio de Janeiro, Brazil
and Depto. de Física, Pont. Univ. Católica, C.P. 38071 BR-22453 Rio de Janeiro, Brazil
and Inst. de Física, Univ. Estadual do Rio de Janeiro, rua São Francisco Xavier 524, Rio de Janeiro, Brazil
[7] Comenius University, Faculty of Mathematics and Physics, Mlynska Dolina, SK-84215 Bratislava, Slovakia
[8] Collège de France, Lab. de Physique Corpusculaire, IN2P3-CNRS, FR-75231 Paris Cedex 05, France
[9] CERN, CH-1211 Geneva 23, Switzerland
[10] Institut de Recherches Subatomiques, IN2P3 - CNRS/ULP - BP20, FR-67037 Strasbourg Cedex, France
[11] Now at DESY-Zeuthen, Platanenallee 6, D-15735 Zeuthen, Germany
[12] Institute of Nuclear Physics, N.C.S.R. Demokritos, P.O. Box 60228, GR-15310 Athens, Greece
[13] FZU, Inst. of Phys. of the C.A.S. High Energy Physics Division, Na Slovance 2, CZ-180 40, Praha 8, Czech Republic
[14] Dipartimento di Fisica, Università di Genova and INFN, Via Dodecaneso 33, IT-16146 Genova, Italy
[15] Institut des Sciences Nucléaires, IN2P3-CNRS, Université de Grenoble 1, FR-38026 Grenoble Cedex, France
[16] Helsinki Institute of Physics, HIP, P.O. Box 9, FI-00014 Helsinki, Finland
[17] Joint Institute for Nuclear Research, Dubna, Head Post Office, P.O. Box 79, RU-101 000 Moscow, Russian Federation
[18] Institut für Experimentelle Kernphysik, Universität Karlsruhe, Postfach 6980, DE-76128 Karlsruhe, Germany
[19] Institute of Nuclear Physics and University of Mining and Metalurgy, Ul. Kawiory 26a, PL-30055 Krakow, Poland
[20] Université de Paris-Sud, Lab. de l'Accélérateur Linéaire, IN2P3-CNRS, Bât. 200, FR-91405 Orsay Cedex, France
[21] School of Physics and Chemistry, University of Lancaster, Lancaster LA1 4YB, UK
[22] LIP, IST, FCUL - Av. Elias Garcia, 14-1$^{o}$, PT-1000 Lisboa Codex, Portugal
[23] Department of Physics, University of Liverpool, P.O. Box 147, Liverpool L69 3BX, UK
[24] LPNHE, IN2P3-CNRS, Univ. Paris VI et VII, Tour 33 (RdC), 4 place Jussieu, FR-75252 Paris Cedex 05, France
[25] Department of Physics, University of Lund, Sölvegatan 14, SE-223 63 Lund, Sweden
[26] Université Claude Bernard de Lyon, IPNL, IN2P3-CNRS, FR-69622 Villeurbanne Cedex, France
[27] Univ. d'Aix - Marseille II - CPP, IN2P3-CNRS, FR-13288 Marseille Cedex 09, France
[28] Dipartimento di Fisica, Università di Milano and INFN-MILANO, Via Celoria 16, IT-20133 Milan, Italy
[29] Dipartimento di Fisica, Univ. di Milano-Bicocca and INFN-MILANO, Piazza delle Scienze 2, IT-20126 Milan, Italy
[30] Niels Bohr Institute, Blegdamsvej 17, DK-2100 Copenhagen Ø, Denmark
[31] IPNP of MFF, Charles Univ., Areal MFF, V Holesovickach 2, CZ-180 00, Praha 8, Czech Republic
[32] NIKHEF, Postbus 41882, NL-1009 DB Amsterdam, The Netherlands
[33] National Technical University, Physics Department, Zografou Campus, GR-15773 Athens, Greece
[34] Physics Department, University of Oslo, Blindern, NO-1000 Oslo 3, Norway
[35] Dpto. Fisica, Univ. Oviedo, Avda. Calvo Sotelo s/n, ES-33007 Oviedo, Spain
[36] Department of Physics, University of Oxford, Keble Road, Oxford OX1 3RH, UK
[37] Dipartimento di Fisica, Università di Padova and INFN, Via Marzolo 8, IT-35131 Padua, Italy
[38] Rutherford Appleton Laboratory, Chilton, Didcot OX11 OQX, UK
[39] Dipartimento di Fisica, Università di Roma II and INFN, Tor Vergata, IT-00173 Rome, Italy
[40] Dipartimento di Fisica, Università di Roma III and INFN, Via della Vasca Navale 84, IT-00146 Rome, Italy
[41] DAPNIA/Service de Physique des Particules, CEA-Saclay, FR-91191 Gif-sur-Yvette Cedex, France
[42] Instituto de Fisica de Cantabria (CSIC-UC), Avda. los Castros s/n, ES-39006 Santander, Spain
[43] Dipartimento di Fisica, Università degli Studi di Roma La Sapienza, Piazzale Aldo Moro 2, IT-00185 Rome, Italy
[44] Inst. for High Energy Physics, Serpukov P.O. Box 35, Protvino, (Moscow Region), Russian Federation
[45] J. Stefan Institute, Jamova 39, SI-1000 Ljubljana, Slovenia and Laboratory for Astroparticle Physics,
Nova Gorica Polytechnic, Kostanjeviska 16a, SI-5000 Nova Gorica, Slovenia,
and Department of Physics, University of Ljubljana, SI-1000 Ljubljana, Slovenia
[46] Fysikum, Stockholm University, Box 6730, SE-113 85 Stockholm, Sweden
[47] Dipartimento di Fisica Sperimentale, Università di Torino and INFN, Via P. Giuria 1, IT-10125 Turin, Italy
[48] Dipartimento di Fisica, Università di Trieste and INFN, Via A. Valerio 2, IT-34127 Trieste, Italy
and Istituto di Fisica, Università di Udine, IT-33100 Udine, Italy
[49] Univ. Federal do Rio de Janeiro, C.P. 68528 Cidade Univ., Ilha do Fundão BR-21945-970 Rio de Janeiro, Brazil
[50] Department of Radiation Sciences, University of Uppsala, P.O. Box 535, SE-751 21 Uppsala, Sweden
[51] IFIC, Valencia-CSIC, and D.F.A.M.N., U. de Valencia, Avda. Dr. Moliner 50, ES-46100 Burjassot (Valencia), Spain
[52] Institut für Hochenergiephysik, Österr. Akad. d. Wissensch., Nikolsdorfergasse 18, AT-1050 Vienna, Austria
[53] Inst. Nuclear Studies and University of Warsaw, Ul. Hoza 69, PL-00681 Warsaw, Poland
[54] Fachbereich Physik, University of Wuppertal, Postfach 100 127, DE-42097 Wuppertal, Germany

# 1 Introduction

The measurement of the branching ratio for the decay $b \to u\ell\bar{\nu}$ provides the most precise way to determine the $|V_{ub}|$ element of the Cabibbo-Kobayashi-Maskawa (CKM) mixing matrix. Evidence for a non-zero value of $|V_{ub}|$ was first obtained [1,2] by observing leptons produced in $B$ decays with momentum above the kinematic limit for $b \to c\ell\bar{\nu}$ transitions. However, extracting $|V_{ub}|$ from the yield of leptons above the $b \to c\ell\bar{\nu}$ endpoint is subject to a large model dependence. More recently, exclusive $B \to \pi\ell\bar{\nu}$ and $B \to \rho\ell\bar{\nu}$ decays were observed and their rates measured [3,4]. But the determination of $|V_{ub}|$ from exclusive semileptonic decays also has a significant model dependence.

The extraction of $|V_{ub}|$ from the distribution of the invariant mass $M_X$ of the hadronic system recoiling against the lepton pair in $B \to X_u\ell\bar{\nu}$ transitions was proposed several years ago [5] and it has recently been the subject of new theoretical calculations [6,7]. There have been two other $|V_{ub}|$ determinations at LEP based on inclusive analysis of semileptonic decays [8]. The method used here starts from the observation that in most $B \to X_u\ell\bar{\nu}$ decays the hadronic system recoiling against the $\ell\bar{\nu}$ has an invariant mass below the charm mass (see Fig. 1). Because a much larger fraction of the total rate is involved, the model dependence when extracting $|V_{ub}|$ from the decay rate to such states is much smaller than when using the decay rate to leptons above the $b \to c\ell\bar{\nu}$ endpoint or that to exclusive final states [6,7].

This paper presents the first determination of $|V_{ub}|/|V_{cb}|$ based mainly on candidate $B$ semileptonic decays with reconstructed hadronic invariant masses below the $D$ mass and enriched in $b \to u$ transitions using the secondary vertex topology and identified kaons and protons. The shape of the lepton energy spectrum in the $B$ rest frame is also used.

Section 2 describes the event preselection, the particle identification, the reconstruction of the hadronic secondary system and of the $B$ energy and direction, and the $b \to u$ enrichment. Section 3 presents the final event sample, the extraction of $|V_{ub}|/|V_{cb}|$, the stability checks, and the evaluation of the systematic errors. Section 4 summarises.

# 2 Data Analysis

The analysis was performed using data collected by the DELPHI detector at LEP at centre-of-mass energies around the $Z^0$ pole between 1993 and 1995, corresponding to $2.8 \times 10^6$ $Z^0$ hadronic decay candidates. The DELPHI detector was described in detail in [9] and its performance was reviewed in [10]. The backgrounds were estimated using samples of $Z^0$ hadronic decays generated with JETSET 7.3 [11] and passed through the full detector simulation. These simulated events corresponded to 4.9 times the data[1] and were evenly divided in order to describe the DELPHI detector response in the different years of data taking. Background $B \to X_c\ell\bar{\nu}$ decays were generated using, for the exclusive modes, form factors based on a relativistic quark model [12].

Events containing signal $B \to X_u\ell\bar{\nu}$ decays were simulated using a dedicated decay generator [13] interfaced with JETSET and passed through the full DELPHI detector simulation. Hadronic final states were produced using a tuned version of the parton shower model. The values of the branching ratios for the exclusive $B \to \pi\ell\bar{\nu}$ and $B \to \rho\ell\bar{\nu}$ decays were forced to those measured by CLEO [3,4]. The probability of producing vector and axial vector resonances was tuned to agree with the measurements of their inclusive cross sections in $Z^0$ decays.

[1] The numbers of simulated events quoted hereafter in this paper have all been renormalised by this factor 4.9 so as to be directly comparable with the numbers of data events quoted

## 2.1 Event Preselection and Reconstruction

Hadronic events were selected using the standard DELPHI criteria [14]. These yielded 2789419 events in the combined 1993-95 data. The sample was enriched in $Z^0 \to b\bar{b}$ events by applying a $b$-tag algorithm based on measurements of the track impact parameters. This algorithm computes the probability for all reconstructed particles to originate from the event primary vertex [15]. This probability was required to be smaller than 0.08 corresponding to an efficiency of 85% for $Z^0 \to b\bar{b}$ and a rejection factor of about 7 for other hadronic decays. Events were divided into two hemispheres by a plane perpendicular to the event thrust axis. Jets were reconstructed using the LUCLUS clustering algorithm [11] with a $d_{join}$ value of 6.0 GeV. Only events with two or three jets were used. For the two most energetic jets in each event, a secondary vertex reconstruction in the jet was performed using those charged particle tracks with significantly large impact parameters. This procedure allowed to inclusively reconstruct a jet secondary vertex in 60% of all the jets in events satisfying the $b$-tagging criteria.

## 2.2 Particle Identification

For this analysis, hadronic $b$-tagged events were required to contain one identified lepton ($e$ or $\mu$). Candidate leptons from semileptonic $B$ decay were selected in the momentum interval 3.5 GeV/c $< p <$ 25 GeV/c.

Muons were identified by the hits associated in the muon chambers. The efficiency was estimated from simulation to be (83.0±2.0)%. The probability for a hadron to be misidentified as a muon was measured on data to be (0.68±0.03)%.

Electron candidates were selected using a Neural Network based on the response of the HPC electromagnetic (e.m.) calorimeter and on the measured specific ionisation ($dE/dx$) in the TPC. The efficiency of this selection criteria was measured with Compton events in data, yielding (70.0±2.0)% with a misidentification probability of (0.38±0.03)%. In order to reduce the background from $b \to c \to \ell$ and $c \to \ell$ transitions the lepton candidates were required to have $p_t^{in} > 0.5$ GeV/c, where $p_t^{in}$ is the momentum transverse to the jet axis reconstructed including the lepton candidate. In order to ensure its accurate extrapolation to the production point, each lepton candidate was required to have at least one associated hit in the silicon Vertex Detector and a positive lifetime-signed impact parameter relative to the primary vertex.

The identification of strange mesons, which are produced in the cascade $b \to c \to s$ decay, was used to reduce the background from charmed $b$ decays. Kaons and protons, with $p > 2.5$ GeV/c, were identified by the combination of the response of the DELPHI Ring Imaging CHerenkov (RICH) detectors and the $dE/dx$ in the TPC [16]. $K_s^0$ were reconstructed in their $\pi^+\pi^-$ decay mode [10], requiring a total momentum larger than 2.5 GeV/$c$.

Candidate $\pi^0 \to \gamma\gamma$ decays were also tagged. At energies up to about 6 GeV, the two photons from the $\pi^0$ decay are separated enough to produce two distinct electromagnetic showers in the e.m. calorimeter. Photon pairs with a total energy below 9 GeV and with an invariant mass 0.045 GeV/c$^2$ $< m_{\gamma\gamma} <$ 0.225 GeV/c$^2$ were accepted as $\pi^0$ candidates. At larger energies, $\pi^0$'s were discriminated from photons by the e.m. cluster shape reconstructed in the HPC calorimeter.

## 2.3 Reconstruction of the Secondary Hadronic System

A total of 52952 hemispheres with an identified lepton were accepted in data and 52661 for the simulated backgrounds.

The secondary hadronic system was reconstructed using an inclusive method. First a likelihood variable was computed as the product of the likelihood ratios that the particle originated from the $B$ decay or from the primary hadronisation for a set of discriminating variables. These were divided into two categories. The first consisted of the following six kinematical variables: transverse momentum $p_t$, ratio of particle momentum and jet energy $p/E_{jet}$, particle mass, rapidity, rank in decreasing energy order, and increase of the invariant mass of the particles associated to the jet secondary vertex by the addition of this particle. These variables were computed for all charged particles with momenta above 0.5 GeV/c and neutral particles with energy above 1.0 GeV. The second category grouped four topological variables computed only for charged particle tracks with $p > 0.7$ GeV/c and associated hits in the Vertex Detector. These variables were the track impact parameters relative to the primary event vertex in the $R-\phi$ and $z$ projections normalised to their errors, the $\chi^2$ contribution of the track to the jet inclusive secondary vertex, and the distance of the point of closest approach of the track to the jet axis normalised to the distance between the primary and secondary vertex.

The hadronic secondary system was then reconstructed via an iterative algorithm that used the charged particles sorted by decreasing value of the above likelihood variable to define a secondary vertex. All charged particles with likelihood larger than 0.75 were tested for their compatibility with originating from a common secondary vertex. Those contributing less than 4.0 to the $\chi^2$ of the secondary vertex fit and giving a total invariant mass $M_X$ smaller than 3.0 GeV/c$^2$ were accepted. After the charged hadronic system was defined, identified $K^0_s$ and $\pi^0$ candidates with a likelihood larger than 0.65 were tested. At most two $\pi^0$'s were accepted at each vertex, if the total invariant mass of the particles associated to the vertex did not exceed 3.0 GeV/c$^2$. Reconstructed secondary hadronic systems with only neutral particles, with an absolute value of the charge above 1, or with a total energy smaller than 4 GeV were rejected. Secondary hadronic systems consisting of a single particle were accepted if the particle was consistent with forming a common vertex with the lepton, in this case the mass $M_X$ was set to the $\pi$ mass. The total and charged multiplicities of the secondary system for data and simulation are shown in Fig. 2. The corresponding energy distributions for the secondary hadronic system $X$, the $X\ell$ system, the missing energy in the hemisphere, and the $X\ell\bar{\nu}$ system are shown in Fig. 3. A secondary hadronic system was reconstructed in 75% of simulated $B \to X_c\ell\bar{\nu}$ decays satisfying the event selection criteria described above, and in 69% of signal $B \to X_u\ell\bar{\nu}$ decays. 37986 decays were reconstructed in the data and 37899 in the simulation.

The total mass of the candidate $B$ decay, $M_{X\ell\bar{\nu}}$, was estimated from the invariant mass of the system formed by the secondary hadronic system, the lepton and the neutrino as discussed below. For $B \to X_u\ell\bar{\nu}$ and fully reconstructed $B \to X_c\ell\bar{\nu}$ decays, $M_{X\ell\bar{\nu}}$ peaks at $\sim 5.0$ GeV/c$^2$ and has a resolution of 0.9 GeV/c$^2$, while for partially reconstructed $B \to X_c\ell\bar{\nu}$ decays $M_{X\ell\bar{\nu}}$ peaks at 4.5 GeV/c$^2$ (see Fig. 4). The latter decays contribute a background at values of $M_X$ below the charm mass. They can be identified in part because of their lower value of $M_{X\ell\bar{\nu}}$ compared with fully reconstructed decays. Therefore, decays with $M_{X\ell\bar{\nu}} < 3.0$ GeV/c$^2$ were removed. For decays with 3.0 GeV/c$^2$ $< M_{X\ell\bar{\nu}} <$ 4.5 GeV/c$^2$ and $M_X < 1.6$ GeV/c$^2$, the measured hadronic mass $M_X$ was rescaled by $M_B/M_{X\ell\bar{\nu}}$. Of the decays in this category that passed the final selections (see Table 1, below), this rescaling promoted 46.2% to $M_X > 1.6$ GeV/c$^2$ in data and 45.8% in simulation. In order to further remove partially reconstructed $D$ decays, all charged particles in

the lepton hemisphere with $p > 1.5$ GeV/c which were not associated with the secondary vertex were tested for their probability to originate at the event primary vertex. Decays giving a probability below 0.025 were removed, since this low probability indicates the presence of additional secondary particles that were not included. In addition, decays with two identified leptons in the same hemisphere were removed, because double semileptonic $B \to X_c \ell \bar{\nu}$, $X_c \to X_s \bar{\ell} \nu$ decays result in a low mass hadronic system and represent a background to this analysis. The secondary hadronic system reconstruction and selection gave 34583 accepted hemispheres in data and 33769 in simulation.

Finally, an inclusive search for $D^* \to D\pi$ was performed. Charged pion candidates with 0.4 GeV/c $< p <$ 3.0 GeV/c and $p_t <$ 0.7 GeV/c and $\pi^0$ candidates with 1.5 GeV $< E <$ 3.0 GeV and $E_t <$ 0.7 GeV were added in turn to the secondary system $X$ and the mass difference $\Delta M = M_{X\pi} - M_X$ was computed. Events with 0.14 GeV/c$^2$ $< \Delta M <$ 0.16 GeV/c$^2$ and a secondary hadronic mass above 0.6 GeV/c$^2$ were accepted as candidate $D^*$ decays. Their mass $M_X$ was then fixed to 2.01 GeV/c$^2$. In the simulation, these criteria correctly identified 44% of semileptonic decays with a $D^*$ meson and $M_X <$ 1.6 GeV/c$^2$. This procedure promoted a further 13.8% to $M_X > 1.6$ GeV/c$^2$ in data, and 14.2% in simulation.

## 2.4 Boosted Lepton Energy

In order to improve the separation of $B \to X_u \ell \bar{\nu}$ from $B \to X_c \ell \bar{\nu}$ and other background sources, the lepton energy in the $B$ rest frame was determined. For each decay, the energy of the $B$ hadron (see Fig. 3) was estimated as the energy sum of the identified lepton, the secondary hadronic system and the neutrino energy. The neutrino energy was computed from the missing energy in the hemisphere corrected by a function of the $E_{X\ell}$ energy determined from the simulation [17]. Neutrino energies in the range of 1.5 GeV $< E_\nu <$ 25 GeV and a minimum $B$ energy of 25 GeV were required. The resolution of the neutrino energy in $B \to X \ell \bar{\nu}$ decays was estimated to be 3.6 GeV. The resulting resolution of the $B$ energy was studied on simulation and found to be 9.8% for 80% of all inclusive semileptonic $B$ decays and 15.4% for the remaining decays. The $B$ direction was taken as the vector joining the primary vertex to the jet secondary vertex. For those decays without a reconstructed secondary vertex, the sum of the momentum vectors of the hadronic system, of the lepton and of the missing momentum was computed. The angular resolution of the $B$ direction was estimated to be 3.2° for semileptonic $B$ decays.

The lepton energy $E_\ell^*$ was computed in the frame defined by the estimated $B$ energy and direction. The resolution on the $E_\ell^*$ reconstruction was studied on simulated events and found to be 14% for 81% of the selected decays. The values of the resolution obtained by analysing $B \to X_u \ell \bar{\nu}$ and $B \to X_c \ell \bar{\nu}$ events separately were found to be consistent.

## 2.5 $b \to u$ enrichment

A procedure was developed to select separate samples, enriched or depleted in $b \to u$ transitions, independently of the reconstructed hadronic mass. It relies on the sign of the lepton impact parameter relative to the secondary vertex position and on the presence of identified kaons in the same hemisphere as the lepton. For each hemisphere, with a reconstructed secondary vertex, the lepton impact parameter $d_{sec}^{\ell}$ was computed relative to this vertex and signed using the lifetime convention, *i.e.* it was signed negative if the lepton appeared to originate between the primary and the secondary vertex, and positive if it was downstream of the secondary vertex. In $B \to X_c \ell \bar{\nu}$ decays, the secondary

vertex corresponds mainly to the charm decay vertex. Consequently, $b \to c$ semileptonic transitions tend to give leptons with negatively signed impact parameters, since the lepton comes from the $B$ decay vertex. But in $B \to X_u \ell \bar{\nu}$ transitions, the secondary vertex coincides with the $B$ decay vertex and thus with the lepton production point, so the impact parameter signing depends only on resolution effects and is positive or negative with equal probability. Therefore, events with a reconstructed secondary vertex and a significantly negative lepton impact parameter were assigned to the $b \to u$ depleted class. Requiring $d^{\ell}_{sec} < -0.015$ cm selected 29.4% of the decays fulfilling the final selection in data, and 28.7% in the simulated background sample. Those with a single secondary particle not identified as a kaon or a proton were assigned to the $b \to u$ enriched class.

The detection of a strange particle in the semileptonic $B$ decay was also used to separate cascade $B \to X_c \ell \bar{\nu}$ followed by $X_c \to K^{\pm} X$ decays from $B \to X_u \ell \bar{\nu}$ transitions, where the production of strange particles is suppressed because they can originate only from the spectator $s$ quark in $B_s$ decays or from the production of an $s\bar{s}$ pair in the hadronisation process. In the same hemisphere as the lepton, 36.5% of reconstructed decays contained an identified $K^{\pm}$, $K^0_s$ or proton in the data, and 37.8% in the simulated backgrounds, while the simulation predicts 14% in $b \to u$ transitions. These decays were assigned to the $b \to u$ depleted class if $d^{\ell}_{sec} < 0$.

# 3 Results

Candidate semileptonic $B$ decays were further selected by imposing the following selection in order to remove background and poorly reconstructed decays. The summed energy of the hadronic system and the lepton was required to be larger than 12 GeV and larger than 70% of the jet energy. Decays with an invariant mass of the secondary hadronic system and of the lepton $M_{X\ell}$ below 2.0 GeV/c$^2$ were also removed. Finally, decays in which the lepton charge had a sign equal to that of the hadronic system were discarded. These criteria selected 12134 decays in data. The $Z^0$ simulated sample, which contained no $b \to u$ transitions, gave 11695 expected events, while from a dedicated signal sample an efficiency for $B \to X_u \ell \bar{\nu}$, with $\ell = e, \mu$, of (9.3$\pm$0.3)% was obtained. The background composition was studied on simulation, for $E^*_{\ell} > 0.8$ GeV, and found to consist of 90% of $B \to X_c \ell \bar{\nu}$ decays, 8% of cascade $B \to X_c \to X_s \bar{\ell} \nu$ decays and 2% of $D \to X_s \bar{\ell} \nu$ decays and misidentified hadrons.

Selected decays were divided into four independent classes according to the reconstructed secondary hadronic mass $M_X$ and the $b \to u$ enrichment criteria, described in section 2.5. These are: i) $b \to u$ enriched decays with $M_X < 1.6$ GeV/c$^2$, ii) $b \to u$ enriched decays with $M_X > 1.6$ GeV/c$^2$, iii) $b \to u$ depleted decays with $M_X < 1.6$ GeV/c$^2$, and iv) $b \to u$ depleted decays with $M_X > 1.6$ GeV/c$^2$. The $M_X$ value of 1.6 GeV/c$^2$ was chosen on the basis of simulation studies. These showed that this value (a) was large enough to ensure a reduced model dependence in the extraction of $|V_{ub}|$ [7,13], (b) was sufficiently below the $D$ mass to suppress the bulk of $B \to X_c \ell \bar{\nu}$ decays, and (c) minimised the statistical error on $|V_{ub}|/|V_{cb}|$.

The numbers of events selected in data, the numbers of expected background events, and the expected fractions of the total number of signal events in the four classes are summarised in Table 1. The background was rescaled by the normalisation factor obtained from the fit described in section 3.1 including the $\pm$0.01 error on this normalisation. For decays selected in the low $M_X$ and $b \to u$ enriched class, which is expected to contain 68% of the $b \to u$ signal, an excess of 214$\pm$56 events above the expected background was found in the data (see Figs. 6,7). No significant excess was observed in the other classes,

where the $\chi^2$ probability of a deviation of the data from the prediction larger than that observed is 30%.

As a cross-check, the analysis was repeated using both anti-$b$-tagged events and decays with same-sign lepton and hadronic vertex combinations. All other selection criteria were kept as in the main analysis. Both these samples are expected to be depleted in signal $b \to u$ decays but they are sensitive to possible discrepancies between data and simulation in the description of backgrounds. The numbers of selected decays in the low $M_X$ and $b \to u$ class were computed. For the anti $b$-tagged sample 32 events were observed in the data compared to 33$\pm$3 expected from background. The same-sign sample consisted of 340 events in data with 317$\pm$8 expected from backgrounds. No excess of events in data was observed in either of these samples.

Table 1: *Numbers of events selected in the data, expected background events, and expected fractions of the total number of signal events. The background is rescaled by the normalisation factor obtained from the fit described in section 3.1, including its* $\pm 0.01$ *error*

| Selection | $b \to u$ enriched | | | $b \to u$ depleted | | |
|---|---|---|---|---|---|---|
| | Data | Back. | Sig. | Data | Back. | Sig. |
| $M_X < 1.6$ GeV/c$^2$ | 2292 | 2078$\pm$30 | 68% | 1081 | 1118$\pm$19 | 9% |
| $M_X > 1.6$ GeV/c$^2$ | 5017 | 5019$\pm$60 | 17% | 3744 | 3618$\pm$46 | 6% |

In order to check the interpretation of the excess of events in the low $M_X$ and $b \to u$ enriched sample as a signal for $B \to X_u \ell \bar{\nu}$ transitions, a search for decays into the $B \to \pi \ell \bar{\nu}$ and $B \to \rho \ell \bar{\nu}$ exclusive final states was performed. Decays with 1.0 GeV $< E_\ell^* <$ 3.0 GeV and a reconstructed hadronic system consisting either of a single charged particle or of two particles with total charge $Q = 0$ or $\pm 1$ were selected. The lepton energy requirement further suppressed the non $B \to X_c \ell \bar{\nu}$ backgrounds. The $M_X$ distribution shows an excess of events in the data compared to the expected backgrounds in good agreement with the expectation from $B \to \pi \ell \bar{\nu}$ and $B \to \rho \ell \bar{\nu}$ exclusive final states (Fig. 8). As a cross-check, the analysis was repeated for same-sign combinations of the lepton and the hadronic system. This class receives signal contributions only from partially reconstructed decays like $B^+ \to \pi^+(\pi^-)\ell^+\nu$, where the $(\pi^-)$ is not reconstructed, and background events. No significant excess of events was observed (see Fig. 8).

## 3.1 Extraction of $|V_{ub}|/|V_{cb}|$

The numbers of events in each decay class and their $E_\ell^*$ distributions were used to determine the value of $|V_{ub}|/|V_{cb}|$ by a simultaneous binned maximum-likelihood fit. The ratio $|V_{ub}|/|V_{cb}|$ is given by the ratio of $X_u \ell \bar{\nu}$ to $X_c \ell \bar{\nu}$ decays through the relationship [18,19]:

$$\begin{aligned} \frac{|V_{ub}|}{|V_{cb}|} = & \frac{0.00445}{0.04110} \times \left( \frac{BR(B \to X_u \ell \bar{\nu}_\ell)}{BR(B \to X_c \ell \bar{\nu}_\ell)} \times \frac{0.105}{0.002} \right)^{1/2} \\ & \times (1 \pm 0.055_{QCD} \pm 0.015_{m_b}) \end{aligned} \quad (1)$$

In the fit, the overall data to simulation normalisation and the value of $|V_{ub}|/|V_{cb}|$ were left free to vary while the non $B \to X_c \ell \nu$ backgrounds were kept fixed to the fractions predicted from the simulation. This significantly reduced the systematic uncertainties from the lepton identification and other sources by absorbing their effects in this overall normalisation factor.

The result of the fit (see Fig. 7) was:

$$|V_{ub}|/|V_{cb}| = 0.103\ ^{+0.011}_{-0.012}\ \text{(stat.)}$$

with the normalisation factor 1.013±0.011.

## 3.2 Stability checks

The stability of the fitted value of $|V_{ub}|/|V_{cb}|$ was checked in various ways. Repeating the analysis for electrons and muons separately gave 0.095±0.017 and 0.107±0.014 respectively. Moving the cut on $M_X$ from 1.6 GeV/c$^2$ to 1.05 GeV/c$^2$ or 1.90 GeV/c$^2$, which changed the signal-to-background ratio from 0.10 to 0.15 or 0.055, changed the fit result to $|V_{ub}|/|V_{cb}| = 0.098\pm0.013$ or $0.105\pm0.013$, respectively. Several other selection criteria were also varied or dropped, including the cuts on event $b$-tagging, lepton $p_t$, $E_{X\ell}$, $M_{X\ell}$, $E_B$ and the secondary vertex decay distance significance, and the results were found to agree within the errors. Removing the scaling of the hadronic invariant mass $M_X$, described in section 2.3, gave 0.105±0.013. Excluding the information on the lepton energy gave 0.106±0.015. Keeping the simulation to data normalisation fixed gave $|V_{ub}|/|V_{cb}| = 0.108\pm0.009$.

Finally, the analysis was repeated with an improved rejection of double semileptonic decays $B \to X_c\ell\bar{\nu}$, $X_c \to X_s\bar{\ell}\nu$. Because of the presence of an additional neutrino and the lower secondary charged particle multiplicity, these decays can be confused with $B \to X_u\ell\bar{\nu}$ transitions. A loose $e$ and $\mu$ identification procedure, based on the $dE/dx$ measured in the TPC, the measured ratio of calorimetric energy to momentum, $E/p$, and the hit pattern in the Hadron Calorimeter, was developed. This had an efficiency of 75% for leptons not already identified by the standard tagging procedure and a hadron misidentification probability of 18% in the momentum range 3 GeV/c $< p <$ 10 GeV/c. Candidate decays were rejected if the secondary charged particle multiplicity (not including the seed high $p_t$ lepton) did not exceed two and at least one secondary particle was tagged as a lepton with these looser requirements. This gave $|V_{ub}|/|V_{cb}| = 0.100\pm0.013$.

## 3.3 Systematic Uncertainties

Four categories of systematic uncertainties were considered. The first three affect primarily the estimation of the large $b \to c$ backgrounds. The fourth affects primarily the evaluation of $|V_{ub}|/|V_{cb}|$ from the observed excess in the $b \to u$-enriched sample. The results for $|V_{ub}|/|V_{cb}|$ are summarised in Table 2.

### 3.3.1 Systematic errors from charm decays

The description of charm decays affects the fraction of $B \to X_c\ell\bar{\nu}$ transitions that were accepted in the $b \to u$ enriched sample. First, the branching fractions for $D$ decays into final states with low charged multiplicity were considered. These are $D \to K^0X$, which in the simulation contributes 40% of the background from $b \to c$ decays in the $b \to u$ enriched sample, and $D$ decays in 0 and 1 prong final states, which contribute 46%. Varying their branching ratios within the uncertainties of the MARK III measurement [20] changed the fitted value of $|V_{ub}|/|V_{cb}|$ by ±0.0062 and ±0.0025, respectively. Varying the ratio of prompt $B$ semileptonic decays to cascade and charm decays by the uncertainty on the ratio BR($b \to \ell$)/BR($c \to \ell$) = (0.106±0.002)/(0.098±0.003) [21] contributed an uncertainty of ±0.0042.

### 3.3.2 Uncertainties in $B$ hadron production and decay

The first component is due to the fraction of $B_s$ and beauty baryons produced. Due to the rejection of kaons and protons associated with the lepton hemisphere these beauty hadrons do not significantly contribute to the $b \to u$ enriched sample. Propagating the uncertainty of $\pm$ 0.020 on the sum of $B_u$ and $B_d$ meson fractions [19] contributed 0.0039. Varying the $\epsilon_b$ parameter in the Peterson $b$ fragmentation function according to the uncertainty in the fraction of the beam energy taken by the beauty hadron, $< x_b >$ = 0.702$\pm$0.008, contributed 0.0010. Varying the inclusive $b$ lifetime by the uncertainty of the present world average, (1.564$\pm$0.014) ps [19], contributed 0.0011. The branching fraction for inclusive double charm production in $B$ decays was fixed to 0.15 and varied by $\pm$0.03. This changed the fit result by $\pm$0.0025. Finally, the dependence on the production rate of $D^*$ and $D^{**}$ mesons (where $D^{**}$ denotes either a non-resonant $D^*\pi$ final state or a $D_J^{(*)}$ higher excited charmed meson state) in $B$ semileptonic decays was studied. These states flip the charge of the resulting $D$ meson and thus increase the charged multiplicity in $b$ hadronic decays. Using the values BR($B \to D^*\ell\bar{\nu}$) = (0.046$\pm$0.003) [22] and BR($B \to D^{**}\ell\bar{\nu}$) = (0.034$\pm$0.006) [23], gave a sum of 0.080$\pm$0.007, corresponding to a contribution to the systematic error of 0.0033. In addition, the amount of non-resonant $D^{(*)}\pi$ states was varied from zero to 50% of the $D^{**}$ yield. This contributes systematic uncertainties both from the shape of the lepton energy spectrum and from the vertex topology and secondary charged multiplicity corresponding to an uncertainty of $\pm$0.0065.

Finally the systematic error from the model of the shape of the lepton spectrum in the background $b \to c$ semi-leptonic transitions was estimated. The lepton spectra observed for the three signal-depleted classes were found to agree with those from the simulation (see Fig. 6). In addition, a sample enriched in $B \to D^*(X)\ell\bar{\nu}$ decays was compared with the simulation prediction and was also found to be in good agreement. The spectrum predicted by the DELPHI simulation program was compared with that from the ISGW-2 model [24] implemented in the EVTGEN decay generator [25]. The relative contributions of the different charm states were set to the central values discussed above in order to be sensitive only to the difference in the predicted shape of the lepton spectrum. The difference of 0.0020 in the fit result was taken as the corresponding contribution to the systematic uncertainty.

### 3.3.3 Detector dependent systematics

The first source is due to the efficiency and purity of the lepton identification. Efficiency and misidentification probability for muon and electron tagging were extracted from both the simulation and data as discussed in 2.2. The central values for the simulation were changed within these errors and the corresponding changes on $|V_{ub}|/|V_{cb}|$ were found to be 0.0015 and 0.0020, respectively.

The second component of detector systematics is due to the hadronic mass and rest-frame lepton energy resolution. The former depends on both the secondary hadronic multiplicity and the single particle energy resolution. The secondary hadronic multiplicity was studied on the $b \to u$ depleted sample to avoid possible biases from the presence of signal events in the data. The total (charged) multiplicity of the secondary hadronic system was measured to be 3.64$\pm$0.01 (2.74$\pm$0.01) in the data and 3.63$\pm$0.01 (2.72$\pm$0.01) in the simulation. The systematic uncertainty was evaluated by considering a change of $\pm$0.02 units of multiplicity. This gave a variation of $|V_{ub}|/|V_{cb}|$ of $\pm$0.0065. The component due to the particle energy resolution is dominated by the resolution of neutral particles. The systematic effects were checked by decreasing by 2% the resolution on $M_X$ for those

decays with neutral particles. This range was defined by a $\chi^2$ analysis of the hadronic mass in real and simulated $b \to u$ depleted decays. It also corresponds to the effect from the electromagnetic energy resolution typically measured in $Z^0$ decays. The corresponding systematic uncertainty was found to be 0.0010. The resolution on the neutrino energy reconstruction was varied by 10% and the effect was propagated to the $E_\ell^*$ resolution, giving a systematic error contribution of 0.0010.

Thirdly, the possible systematics in the decay classification were studied. These systematics depend both on the measurement and sign of the lepton impact parameter relative to the secondary vertex and on the kaon identification. The lepton impact parameter systematic has two components. The first is due to the lepton extrapolation and the second to the secondary vertex reconstruction. The effect of changing the resolution on the lepton track extrapolation was computed by smearing the resolution on the lepton impact parameter by 5%, which corresponds to the maximum discrepancy observed in the resolution functions obtained in data and in simulation [26]. The component due to the secondary vertex position was evaluated by smearing the resolution on its decay length by 50 $\mu$m, which corresponds to the additional smearing that increases by one the $\chi^2$ of a data-to-simulation comparison of the decay distance distributions. Summing these two effects in quadrature gave a systematic uncertainty of $\pm 0.0070$. The kaon tagging efficiency was varied by $\pm 2.5\%$, corresponding to the largest observed deviation of the performance of the hadron identification tagging in data and simulation, and the corresponding uncertainty on the result of the fit was 0.0025.

Finally, the statistical error on the efficiency for selecting signal events contributes $\pm 0.0015$ to the systematic uncertainty.

### 3.3.4 Uncertainties in the $B \to X_u \ell \bar{\nu}$ model

The predicted shape of the invariant-mass distribution in the $B \to X_u \ell \bar{\nu}$ decay, depends mainly on the kinematics of the heavy and spectator quarks inside the $B$ hadron and on the $b$ quark mass. Further, the hadronisation process, transforming the $u\bar{q}$ system into the observable hadronic final state, represents an additional source of model uncertainties. These uncertainties were studied using a dedicated generator that implements different prescriptions for the initial state kinematics and the resonance decomposition of the hadronic final states [13].

Varying the $b$ quark mass by $\pm 100$ MeV/$c^2$ [18,27,28], gave a systematic error of $\pm 0.0045$. The value of the $b$ quark mass introduces also an uncertainty in the extraction of $|V_{ub}|/|V_{cb}|$ from the observed $B \to X_u \ell \bar{\nu}$ rate [18,27], see Eq. 1. This gives a total error contribution of 0.0047. The average kinetic energy of the $b$ quark in the hadron, $< p_b^2 >$, has been evaluated both from theory and from fits to experimental data. Results are scheme or model dependent and depend on the method used in their derivation, but point to the value of the parameter $\mu_\pi^2 = (0.5 \pm 0.1)$ GeV$^2$. This variation contributes $\pm 0.0015$ from the uncertainty on the hadronic mass spectrum and $\pm 0.0024$ from the derivation of the ratio $|V_{ub}|/|V_{cb}|$, giving a total of $\pm 0.0028$. The description of the motion of the $b$ quark inside the heavy hadron also contributes uncertainties. The momentum distributions from the ACCMM model [29], a shape function [30,31] parametrised as $f(z) = z^a(1-cz)e^{-cz}$, and the parton model [32] were compared. For the ACCM, the $b$ quark pole mass was kept fixed at its central value of $m_b = 4.82$ GeV/c$^2$ and the $p_F$ value and the $a$ and $c$ coefficients in the QCD structure function were chosen to reproduce the same value of $< p_b^2 >$. For the parton model, the Peterson form [33] of the fragmentation function was adopted with $\epsilon_b = 0.0040$. A systematic uncertainty of $\pm 0.0025$ was evaluated.

Table 2: *Summary of the systematic uncertainties on* $|V_{ub}|/|V_{cb}|$.

| Source | Value ± Range | Syst. Error |
|---|---|---|
| BR($D \to K^0 X$) | $0.53 \pm 0.05$ | 0.0062 |
| BR($D \to 0,1$ prong) | $0.22 \pm 0.02$ | 0.0025 |
| B($b \to \ell$)/BR($c \to \ell$) | $\frac{0.106 \pm 0.002}{0.098 \pm 0.003}$ | 0.0042 |
| Charm decay sub-total | | 0.0079 |
| $f(B_u) + f(B_d)$ | $0.802 \pm 0.020$ | 0.0039 |
| $< x_b >$ | $0.702 \pm 0.008$ | 0.0010 |
| $b$ lifetime | $1.564 \pm 0.014$ | 0.0011 |
| BR($b \to c\bar{c}s$) | $0.15 \pm 0.03$ | 0.0025 |
| BR($B \to D^* \ell\bar{\nu} + D^{**} \ell\bar{\nu}$) | $0.080 \pm 0.007$ | 0.0033 |
| BR($B \to D^{(*)} \pi \ell\bar{\nu}$/BR($B \to D^{**} \ell\bar{\nu}$) | $0.25 \pm 0.25$ | 0.0065 |
| Lepton spectrum shape | | 0.0020 |
| B production and decay sub-total | | 0.0090 |
| $e$ / $\mu$ id. Efficiency | ±2.5% | 0.0015 |
| $e$ / $\mu$ id. Purity | ±10% / ±4.5% | 0.0020 |
| Hadronic Multiplicity | | 0.0065 |
| Neutral Energy Resolution | | 0.0010 |
| Missing Energy Resolution | | 0.0010 |
| $\ell$ Impact Parameter | | 0.0070 |
| $K$ id. Efficiency | ±2.5% | 0.0025 |
| Signal Efficiency | ± 3.0% | 0.0015 |
| Detector-dependent sub-total | | 0.0104 |
| $m_b$ | $4.82 \pm 0.10$ | 0.0047 |
| $< p_b^2 >$ | $0.5 \pm 0.1$ | 0.0028 |
| $b$ Kinematic Model | | 0.0025 |
| Hadronisation Model | | 0.0060 |
| QCD corrections | | 0.0050 |
| $b \to u$ model sub-total | | 0.0099 |
| **Total** | | **0.0186** |

The production of the hadronic final states from the $u\bar{q}$ pair was simulated according to both the ISGW-2 [24] exclusive and a fully inclusive model based on parton shower fragmentation [11]. The ISGW-2 model approximates the inclusive $B \to X_u \ell\bar{\nu}$ decay width by the sum over resonant final states, taking into account leading corrections to the heavy quark symmetry limit. The predicted branching ratios for the different resonant final states were used to define the hadronic system emitted with the lepton. Another approach is to assume that, at sufficiently large recoil $u$ quark energies, the $u\bar{q}$ system moves away fast enough to resemble the evolution of a jet initiated by a light quark $q$ in $e^+e^- \to q\bar{q}$ annihilation. This was simulated by first arranging the $u\bar{q}$ system in a string configuration and then requiring it to fragment according to the parton shower model. Due to the extreme assumptions of the two models adopted, the resulting difference of 0.0160 in the fitted value of $|V_{ub}|/|V_{cb}|$ was assumed to correspond to a 90% confidence region and the $\pm 1\sigma_{syst}$ was estimated to be ±0.0060.

Additional sources of theoretical systematics, arising from the perturbative part of the evaluation and the contribution of non perturbative corrections of order $1/m_b^3$ contribute a $\pm 0.0050$ systematic error [18].

# 4 Summary and Discussion

The value of the ratio $|V_{ub}|/|V_{cb}|$ was measured using a novel technique. The technique uses the reconstructed mass $M_X$ of the secondary hadronic system produced in association with an identified lepton in the semi-leptonic decay of a $B$ hadron and the rest-frame energy spectrum of that lepton. The $b \to u$ signal is enriched using identified kaons and protons and the lepton impact parameter with respect to the secondary vertex. The result obtained is

$$|V_{ub}|/|V_{cb}| = 0.103\ ^{+0.011}_{-0.012}\ \text{(stat.)}\pm 0.016\ \text{(syst.)}\ \pm\ 0.010\ \text{(model)}.$$

Here the systematic error quoted combines the charm decay, B production and decay, and detector-dependent systematics evaluated above, which all primarily affect the estimation of the $b \to c$ backgrounds, and the $b \to u$ model uncertainty is quoted separately. The technique adopted in this analysis allowed both sources of systematic uncertainty to be reduced. At the critical points of the analysis, the behaviour of the data agrees well with the expectations from the simulation. The result is found to be stable with respect to variations in the analysis procedure.

There remains a possible further model dependence arising from a biased sampling of the decay phase space in $B \to X_u \ell \bar{\nu}$ transitions. The stability of the result when the $M_X$ cut was moved from 1.6 GeV/c$^2$ down to 1.05 GeV/c$^2$ or up to 1.90 GeV/c$^2$ (section 3.2) argues against this. To further check this possibility, the relative weights of different regions in the $M_X - E_\ell^*$ plane were analysed. Four regions of the $M_X - E_\ell^*$ plane were defined by selecting decays with $M_X$ and $E_\ell^*$ above and below 0.8 GeV/c$^2$ and 1.75 GeV, respectively. The fit was repeated separately for these four regions. The statistical weights of the four regions are given in Table 3. The result agrees with the expectation of a higher contribution from charmless semileptonic $B$ decays in the low-mass, high-energy and high-mass, low-energy regions and indicates no strong bias in the weighting of the decay phase space.

Table 3: *The weights of the four regions in the $M_X$-$E_\ell^*$ plane, used to check the phase space sampling in the determination of $|V_{ub}|/|V_{cb}|$.*

| | $0.1< M_X <0.8$ GeV/$c^2$ | $0.8< M_X <1.6$ GeV/$c^2$ |
|---|---|---|
| $1.75< E_\ell^* <3.0$ GeV | 0.33 | 0.21 |
| $0.1< E_\ell^* <1.75$ GeV | 0.15 | 0.29 |

While this analysis extracted the ratio of CKM elements $|V_{ub}|/|V_{cb}|$ from the fitted fraction of candidate $B \to X_u \ell \bar{\nu}$ decays, it is also interesting to extract explicitly the the charmless semileptonic branching ratio. This was obtained from the fitted result, assuming $|V_{cb}| = (38.4\pm 3.3) \times 10^{-3}$ and $\tau_b = (1.564\pm 0.014)$ ps [19]. The result was:

$$\begin{aligned}\text{BR}(B \to X_u \ell \bar{\nu}) = (&1.57\pm 0.35\ \text{(stat.)}\pm 0.48\ \text{(syst.)}\pm 0.20\ (|V_{cb}|)\ \pm\ 0.01\ (\tau_b)\\ &\pm\ 0.27\ \text{(model)})\times 10^{-3} \times (|V_{cb}|/0.0384)^2.\end{aligned}$$

where the contribution of correlated model systematics in the derivation of $|V_{ub}|$ and $|V_{cb}|$ was taken into account.

## Acknowledgments

We would like to thank I. Bigi, N. Uraltsev and M. Neubert for discussions on the modelling of the $B \to X_u \ell \bar{\nu}$ decays and on the related systematics in the extraction of $|V_{ub}|/|V_{cb}|$ and D. Lange and A. Ryd for providing an implementation of the ISGW-2 model in the simulation of semileptonic $B$ decays.
We are greatly indebted to our technical collaborators, to the members of the CERN-SL Division for the excellent performance of the LEP collider, and to the funding agencies for their support in building and operating the DELPHI detector.
We acknowledge in particular the support of
Austrian Federal Ministry of Science and Traffics, GZ 616.364/2-III/2a/98,
FNRS–FWO, Belgium,
FINEP, CNPq, CAPES, FUJB and FAPERJ, Brazil,
Czech Ministry of Industry and Trade, GA CR 202/96/0450 and GA AVCR A1010521,
Danish Natural Research Council,
Commission of the European Communities (DG XII),
Direction des Sciences de la Matière, CEA, France,
Bundesministerium für Bildung, Wissenschaft, Forschung und Technologie, Germany,
General Secretariat for Research and Technology, Greece,
National Science Foundation (NWO) and Foundation for Research on Matter (FOM), The Netherlands,
Norwegian Research Council,
State Committee for Scientific Research, Poland, 2P03B06015, 2P03B1116 and SPUB/P03/178/98,
JNICT–Junta Nacional de Investigação Científica e Tecnológica, Portugal,
Vedecka grantova agentura MS SR, Slovakia, Nr. 95/5195/134,
Ministry of Science and Technology of the Republic of Slovenia,
CICYT, Spain, AEN96–1661 and AEN96-1681,
The Swedish Natural Science Research Council,
Particle Physics and Astronomy Research Council, UK,
Department of Energy, USA, DE–FG02–94ER40817.

# References


[1] R. Fulton *et al.* (CLEO Collaboration), *Phys. Rev. Lett.* **64** (1990), 16.
[2] H. Albrecht *et al.* (ARGUS Collaboration), *Phys. Lett.* **B 234** (1990), 409.
[3] J.P. Alexander *et al.* (CLEO Collaboration), *Phys. Rev. Lett.* **77** (1996), 5000.
[4] B.H. Behrens *et al.* (CLEO Collaboration), *Phys. Rev.* **D 61** (2000), 052001.
[5] V. Barger, C.S. Kim and R.J.N. Phillips, *Phys. Lett.* **B 251** (1990), 629.
[6] A.F. Falk, Z. Ligeti and M.B. Wise, *Phys. Lett.* **B 406** (1997), 225.
[7] I. Bigi, R.D. Dikeman and N. Uraltsev, *Eur. Phys. J.* **C 4** (1998), 453.
[8] M. Acciarri *et al.* (L3 Collaboration), *Phys. Lett.* **B 436** (1998) 174;
R. Barate *et al.* (ALEPH Collaboration), *Eur. Phys. J.* **C6** (1999) 555.
[9] P. Aarnio *et al.* (DELPHI Collaboration), *Nucl. Instr. and Meth.* **A303** (1991), 233.
[10] P. Abreu *et al.* (DELPHI Collaboration), *Nucl. Instr. and Meth.* **A378** (1996), 57.
[11] T. Sjöstrand, *Comp. Phys. Comm.* **82** (1994), 74.
[12] M. Bauer, B. Stech and M. Wirbel, *Z. Phys.* **C23** (1985), 637.
[13] M. Battaglia, *Study of $b \to u\ell\nu$ Decays with an Inclusive Generator*, DELPHI 98-42 PHYS 772, hep-ex/0002040.
[14] P. Abreu *et al.* (DELPHI Collaboration), *Phys. Lett.* **B 312** (1993) 253.
[15] P. Abreu *et al.*, (DELPHI Collaboration), *Zeit. Phys.* **C 70** (1996) 531.
[16] M. Battaglia and P.M. Kluit, *Nucl Instr. and Meth.* **A 433** (1999) 252.
[17] P. Abreu *et al.* (DELPHI Collaboration), *Zeit. Phys.* **C 71** (1996), 539.
[18] N. Uraltsev *et al.*, *Eur. Phys. J.* **C 4** (1998), 453 and
N. Uraltsev, *Int. J. Mod. Phys.* **A 14** (1999) 4641.
[19] The ALEPH, CDF, DELPHI, L3, OPAL and SLD Collaborations, *Combined results on b-hadron production rates, lifetimes, oscillation and semileptonic decays*, LEPHF-S Note 99-02.
[20] D. Coffmann *et al.* (Mark III Collaboration), *Phys. Lett.* **B 263** (1991), 135.
[21] The ALEPH, DELPHI, L3, OPAL and SLD Collaborations, *A Combination of Preliminary Electroweak Measurements and Constraints on the Standard Model*, CERN EP-2000-016.
[22] Particle Data Group, *Eur. Phys. J.* **C 3** (1998),1.
[23] P. Abreu *et al.*, (DELPHI Collaboration), CERN-EP/99-174, to appear on *Phys. Lett.* **B**.
[24] D. Scora and N. Isgur, *Phys. Rev.* **D 52** (1995), 2783.
[25] A. Ryd and D. Lange, in Proc. of the *Int. Conf. on Computing in High Energy Physics - CHEP98*, Chicago (USA), September 1998.
[26] P. Abreu *et al.*, (DELPHI Collaboration), *Eur. Phys. J.* **C10** (1999), 415.
[27] A.H. Hoang, Z. Ligeti and A.V. Manohar, *Phys. Rev. Lett.* 82 (1999), 277 and
A.H. Hoang, Z. Ligeti and A.V. Manohar, *Phys. Rev.* D 59 (1999), 074017.
[28] M. Beneke and A. Signer, *Phys. Lett.* **B 471** (1999), 233.
[29] G. Altarelli *et al.*, *Nucl. Phys.* **B 208** (1982), 365.
[30] R.D. Dikeman, M. Shifman and N.G. Uraltsev, *Int. J. Mod. Phys.* **11** (1996), 571.
[31] M. Neubert, *Phys. Rev.* **D 49** (1994), 4623 and
*Phys. Rev.* **D 50** (1994), 2037.
[32] A. Bareiss and E.A. Paschos, *Nucl. Phys.* **B 327** (1989), 353.
[33] C. Peterson *et al.*, Phys. Rev. **D 27** (1983), 105.

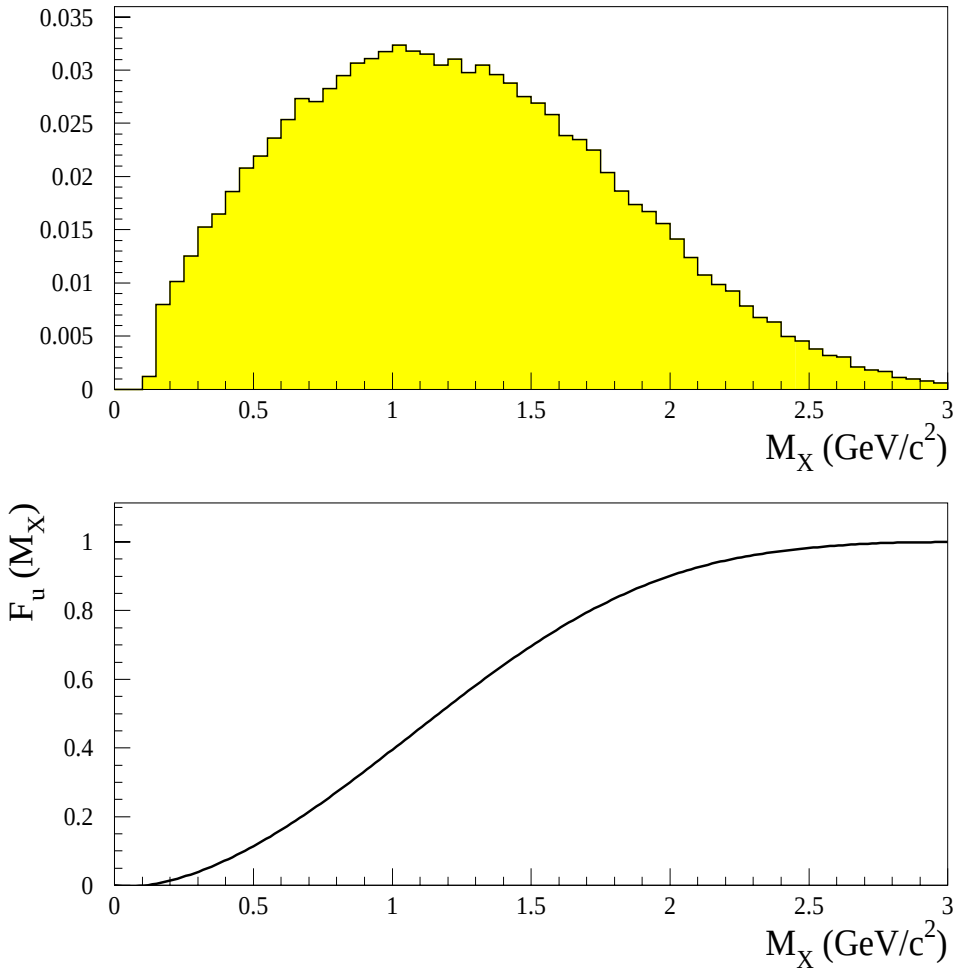


Figure 1: *The invariant mass spectrum $M_X$ of the u-spectator quark system for inclusive $B \to X_u \ell \bar{\nu}$ decays at the parton level obtained with a dedicated decay generator [13] (upper plot) and the fraction of the decays with $M_X$ below a given value (lower plot).*

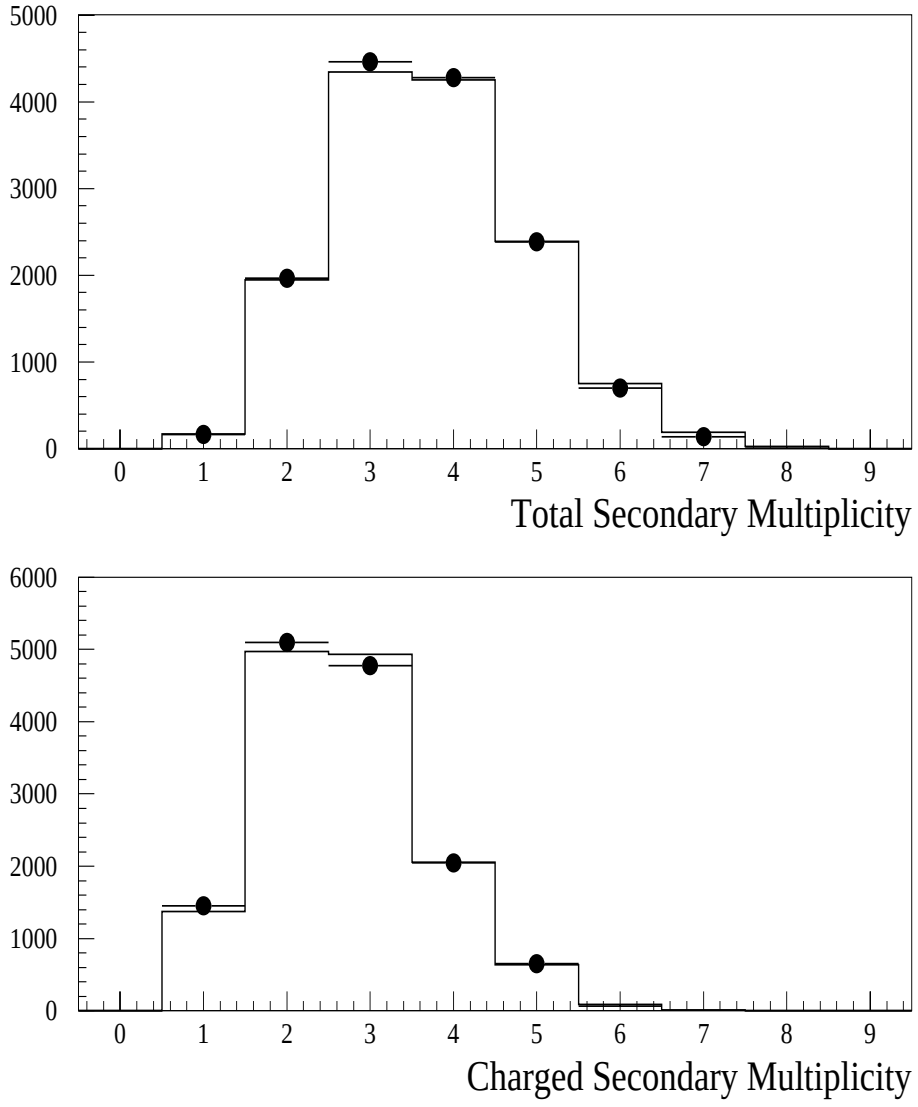


Figure 2: *The total (upper plot) and charged (lower plot) multiplicity of the reconstructed secondary hadronic system in selected decays for data (points with error bars) and simulation (histogram).*

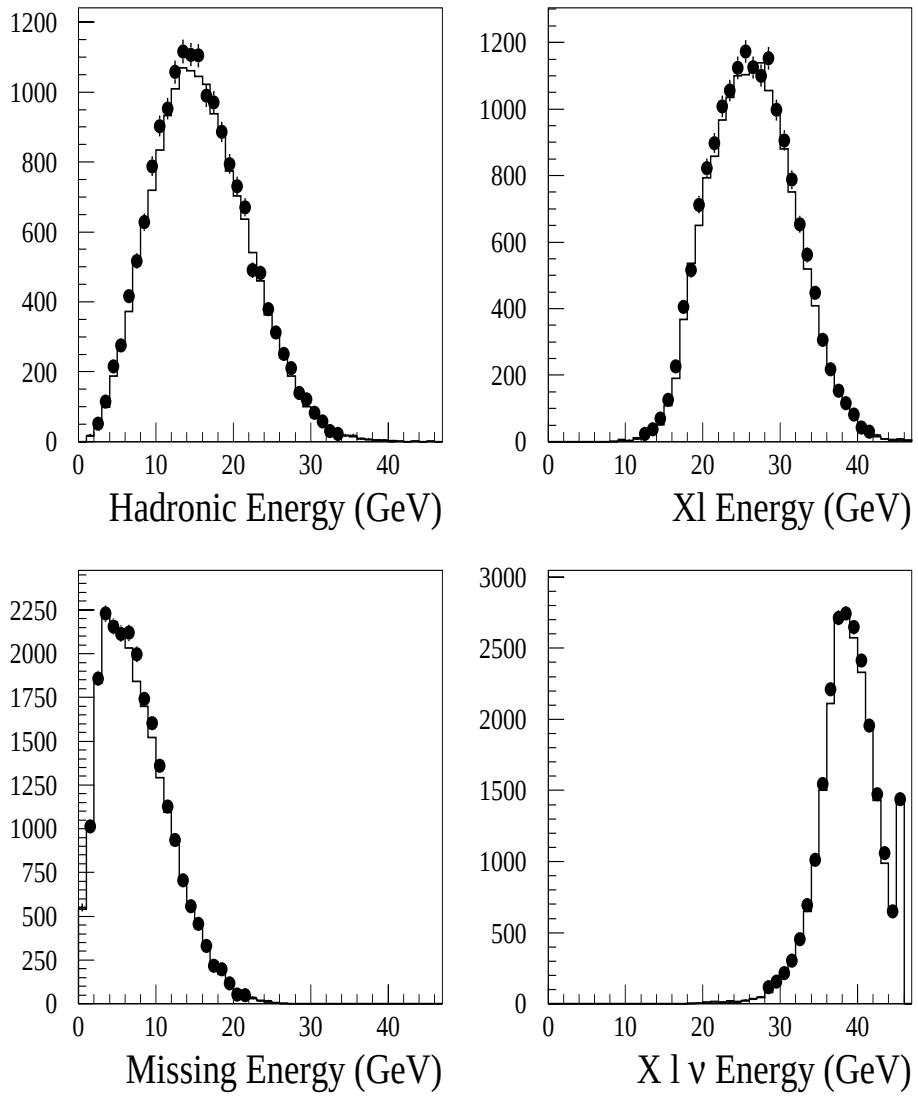


Figure 3: *Energy Distributions: i) energy of the hadronic system (upper left plot), ii) energy of the hadronic system plus the lepton (upper right plot), iii) missing energy (lower left plot) and iv) reconstructed B energy (lower right plot). The dots with error bars represent the data and the histograms the simulation.*

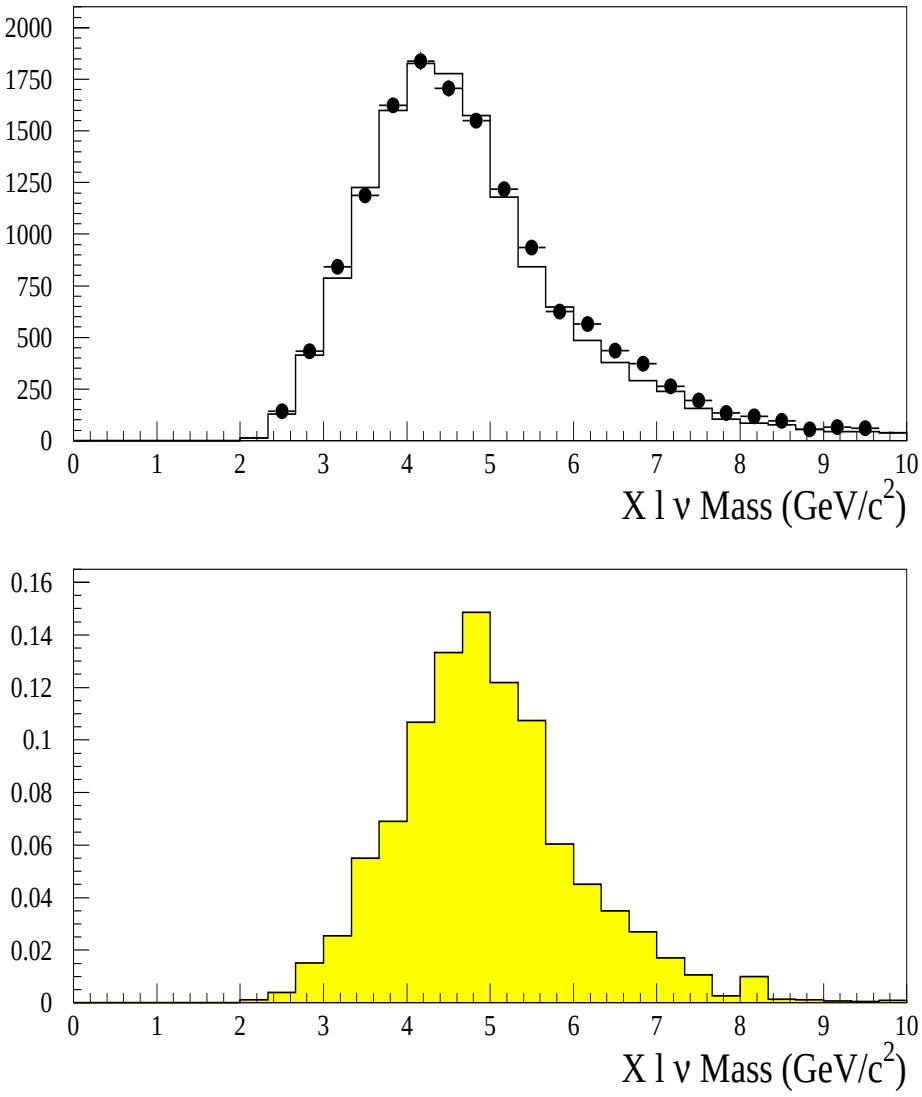


Figure 4: *Invariant mass $M_{X\ell\bar{\nu}}$ of the reconstructed $B$ decay: data (points with error bars) and simulated background (histogram) (upper plot) and $b \to u$ simulated signal (lower plot).*

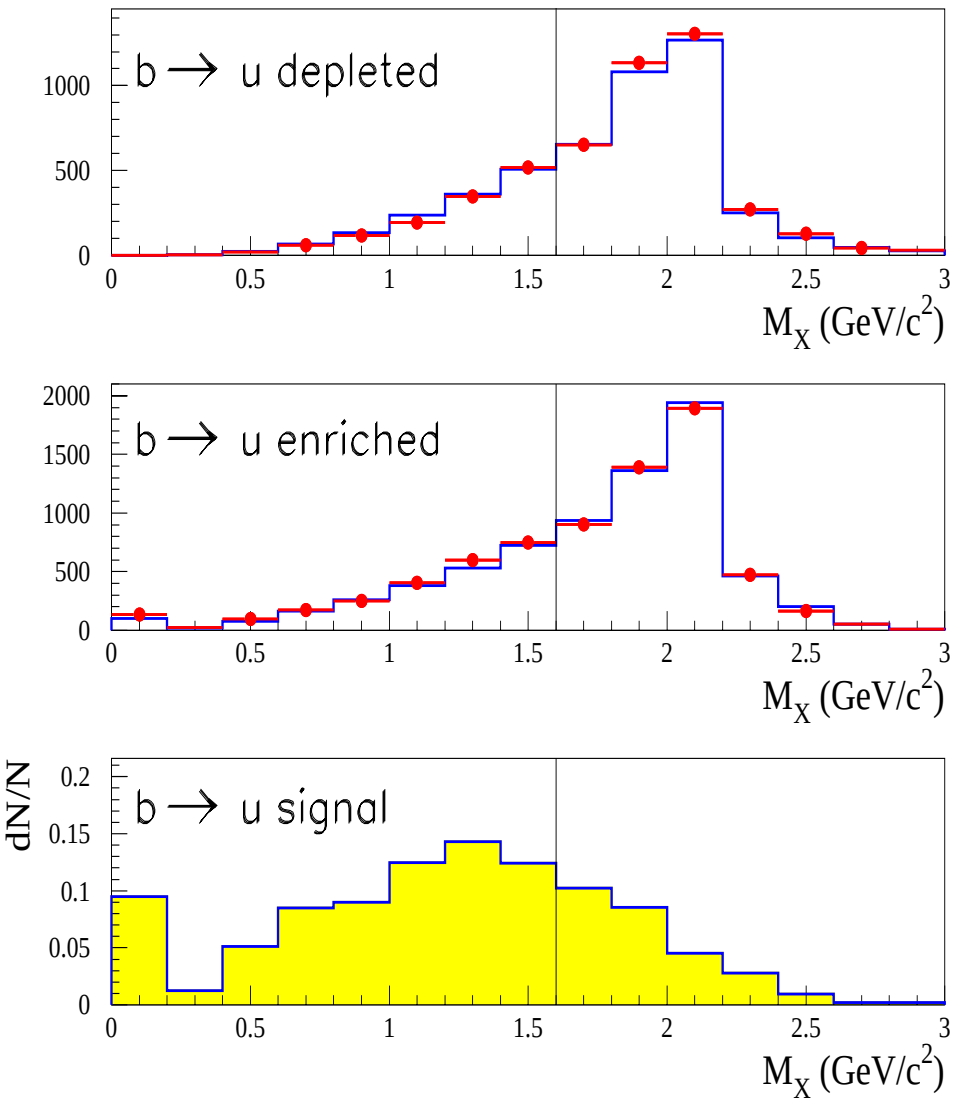


Figure 5: *Invariant mass $M_X$ of the reconstructed secondary hadronic system in selected decays for data (points with error bars) and simulation (histogram). The plots show the $b \to u$ depleted sample (upper plot), the $b \to u$ enriched sample (medium plot) and the $b \to u$ signal (lower plot). The vertical lines correspond to the value chosen for the low $M_X$ selection.*

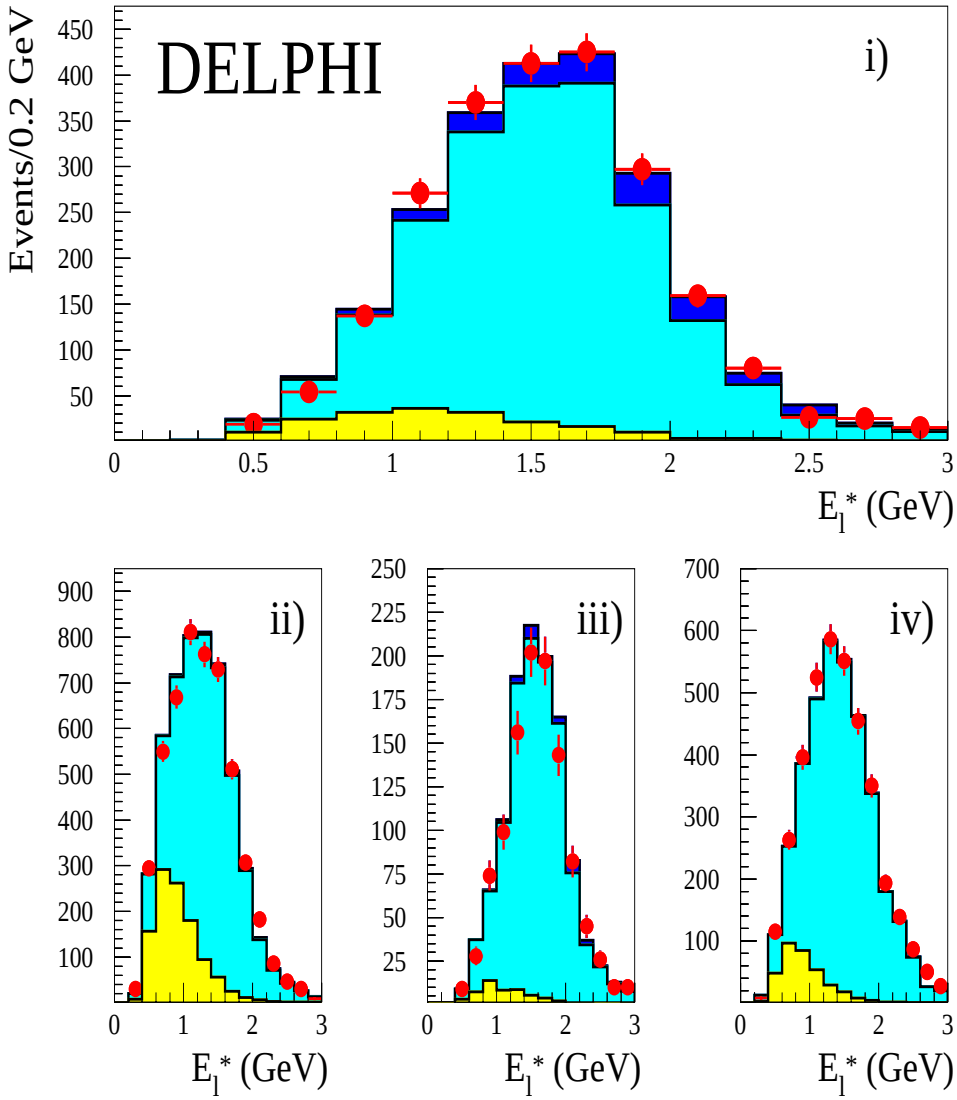


Figure 6: *The $E_\ell^*$ distribution for the decays in the four selected classes: i) $b \to u$ enriched decays with $M_X < 1.6$ GeV/$c^2$ (upper plot), ii) $b \to u$ enriched decays with $M_X > 1.6$ GeV/$c^2$ (lower left), iii) $b \to u$ depleted decays with $M_X < 1.6$ GeV/$c^2$ (lower central plot), and iv) $b \to u$ depleted decays with $M_X > 1.6$ GeV/$c^2$ (lower right plot). Data are indicated by the points with error bars, the $b \to X_u \ell \bar{\nu}$ signal by the dark shaded histograms, the $b \to X_c \ell \bar{\nu}$ background by the medium shaded histograms, and the other backgrounds by the light shaded histograms.*

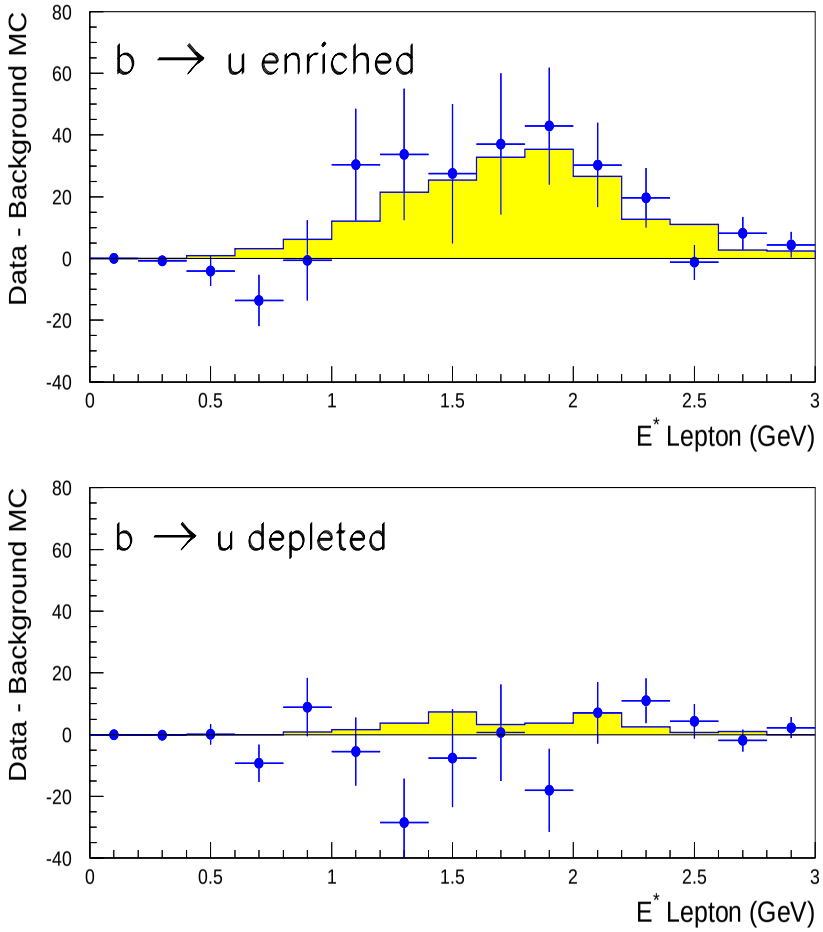


Figure 7: *Background subtracted $E_\ell^*$ distributions: the $b \to u$ enriched decays with $M_X < 1.6$ GeV/$c^2$ (upper plot) and $b \to u$ depleted decays with $M_X < 1.6$ GeV/$c^2$ (lower plot). The background was rescaled by the fitted normalisation factor. The shaded histograms show the expected $E_\ell^*$ distribution for signal $B \to X_u \ell \bar{\nu}$ decays normalised to the amount of signal corresponding to the fitted $|V_{ub}|/|V_{cb}|$ value.*

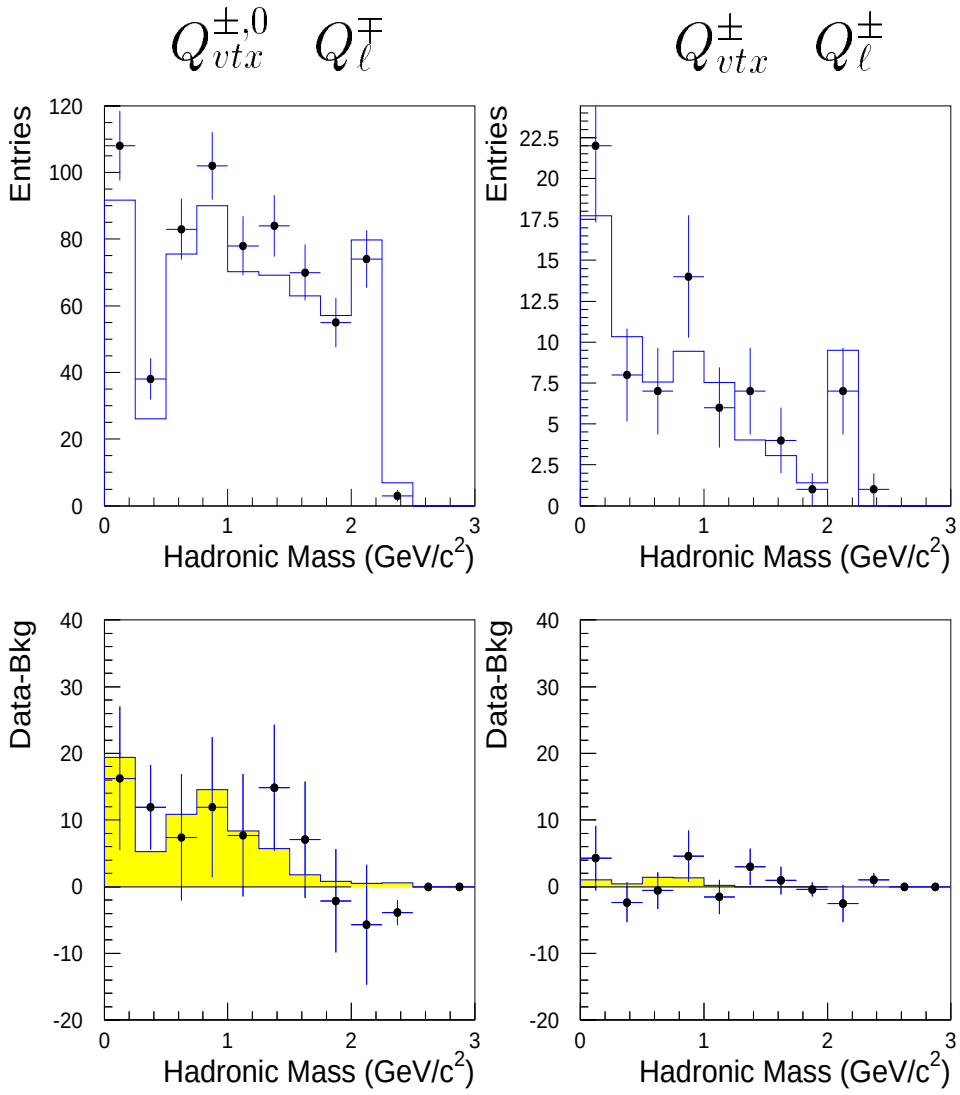


Figure 8: *Invariant mass $M_X$ distributions for $b \to u$ enriched decays with a secondary hadronic system consisting of either a single charged particle or two particles forming a neutral or unit-charge secondary system for opposite sign and neutral-charge (left plots) and same-sign (right plots) hadronic-lepton system. The upper histograms show the expected distribution from backgrounds, the points with error bars the data. In the lower histograms the background subtracted data are compared with the expected distribution from signal $B \to X_u \ell \bar{\nu}$ events.*